JOURNAL OF MATERIALS SCIENCE **40** (2005) 1725–1729

Lamellar structure and twist boundary of NaV_2O_5 grown by flux method

Y. G. WANG*, H. Y. WU
National Laboratory for Condensed Matter Physics, Institute of Physics and Center for Condensed Matter Physics, Chinese Academy of Sciences, P.O. Box 2724, Beijing 100080, People's Republic of China
E-mail: ygwang@blem.ac.cn

V. P. DRAVID
Department of Materials Science and Engineering, Northwestern University, Evanston, Illinois 60208, USA

Microstructures of NaV_2O_5 prepared using flux method were characterized. These structures were observed to be dominated by lamellae with an average thickness of ~1 micron. These lamellae share (001) plane and stack along [001] direction. A small orientation difference among these lamellae was detected with electron diffraction to be within several degrees. A pure twist boundary with (001) plane as the boundary interface and high sigma value of 235 was determined. Within the lamellae there are numerous dislocations arranged parallel to the twist boundary. The twist boundaries and dislocations may introduce distortion in the layers of VO_5 pyramids, which is believed to be unfavorable for Na atoms to position between these layers and may result in non-stoichiometry locally at the boundary.

1. Introduction

Vanadium oxides are found to have many different structures and therefore different electromagnetic properties [1–5]. One of the more remarkable structures is NaV_2O_5. This oxide is of significant importance in that its unique quantum nature exhibits a low-dimensional system with $S = 1/2$ chain and a single ground state and a spin-Peierls transition at the temperature of 35 K. This transition temperature of 35 K is higher than those of $CuGeO_3$ (18 K), Gd_3RuO_7 (14 K), and $CuSiO_3$ (8 K) [6–10]. Carpy and Galy believe that the structure of NaV_2O_5 played a key role in the spin-Peierls transition because they interpret the transition at 35 K as a spin-Peierls transition based on structural change [1]. In their non-centrosymmetric model, a magnetic $V^{4+}O_5$ square pyramid isolated by nonmagnetic $V^{+5}O_5$ square pyramids results in an one dimensional $S = 1/2$ V^{+4} anti-ferromagnetic Heisenberg linear chain that could cause the observed Bonner-Fisher-like temperature dependence in magnetic susceptibility and a spin-Peierls transition at low temperature [7, 11]. Recently, Meetsma and his co-workers re-determined the structure of NaV_2O_5 and reported a centrosymmetric structure [12], which was confirmed by Tsuda *et al.* [13]. In their model for the NaV_2O_5 structure, there is only one type of V site. This implies that all the vanadium sites have a uniform valency of +4.5 above the transition temperature. The phase transition at 35 K is not an ordinary spin-Peierls transition but a spin-charge-lattice-coupled system [14–15].

The aim of this study is to characterize the microstructure of NaV_2O_5 prepared by flux method for a better understanding of the process-microstructure-properties interrelations. We have revealed the lamellar structure with the (001) boundary planes.

2. Experimental details

V_2O_3, V_2O_5 and $NaVO_3$ were used as raw materials for preparation of NaV_2O_5 by flux method. They were mixed in a nominal atomic ratio of 1:1:4 and made compact. The mixture was melted in a platinum crucible at 1273 K, then slowly cooled to 1020 K at a rate of 1 K/h and held at this temperature for 2 days using argon with 5 at% $NaVO_3$ as flux. The obtained NaV_2O_5 crystal is plate-shaped with a longer edge of 2 cm. Finally the NaV_2O_5 was boiled with water to remove any remaining $NaVO_3$ [7]. The transition temperature was measured to be 35 K using NMR and far infrared spectroscopy.

Cross section and plan view TEM specimens were prepared using a modified dimpling/ion milling procedure. Cross section samples allow direct observation of microstructure alternation during crystal growth with high resolution and simultaneous collection of crystallographic information. To prepare cross section

*Author to whom all correspondence should be addressed.

samples, a plate-shaped NaV_2O_5 sample was glued in between two sapphire fillers using M-bone and cured at 400 K in an electric oven to form a raft-like structure. Disks with a diameter of 3 mm were cut with a supersonic cutter, followed by mechanical grinding and dimpling and finally ion thinning to electron transparency using a Gatan dual ion milling system. Plan view samples were made following nearly the same procedures as for cross-section samples but with the plate normal coincident with the electron projected direction. The prepared samples were examined using a Hitachi H-8100 and Phillips CM-200 TEMs equipped with a field emission gun operating at 200 kV.

3. Results and discussion

3.1. Morphology and centrosymmetry of NaV_2O_5

Fig. 1 is a bright-field image at low magnification showing a typical morphology of NaV_2O_5 viewed along [100] direction. Lamellar structures are observed to be well developed along the [001] direction and with an average width of $\sim$1 μm. The grain boundary coincides with the (001) plane. Within the lamellae there are numerous defects extending approximately along [010] direction and piling up in the direction parallel to the grain boundary. The density of these defects is measured to be about 10^6 cm^{-2} and their size in the range of 0.1 to several microns. The small orientation difference among the lamellae was detected with electron diffraction to be within several degrees. As a result the twist boundaries may be introduced between these lamellae.

Large-angle electron diffraction experiment was carried out for quick scan of the whole inverse space. The reconstructed reciprocal space has an orthorhombic symmetry that corresponds to a unit cell with respective lattice parameters of 1.13, 0.360, and 0.45 nm in real space. The deduced extinction of the reflections coincides with two space groups $P2_1mm$ and Pmmn. The difference between them is an inversion center present in Pmmn, but not in $P2_1mm$. Tsuda *et al*. [13] determined an inversion center in NaV_2O_5 using CBED based on the symmetry of a pair of dark-field patterns whose reflection indices have opposite signs [16, 17]. Fig. 2a and b shows the dark-field patterns of the $0\bar{1}\bar{3}$ and 013 reflections, obtained at the exact Bragg angle positions. The contrast distribution in the $0\bar{1}\bar{3}$ diffraction disc is identical with that of the 013 disc, which indicates the presence of an inversion center in the specimen. Therefore it can be concluded that NaV_2O_5 has centrosymmetry and the correct space group is Pmmn.

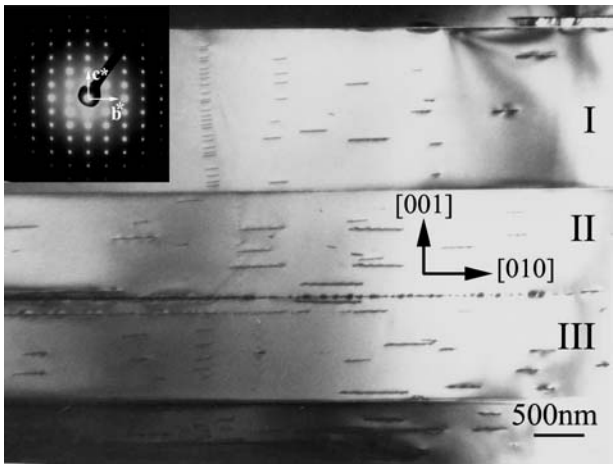

Figure 1 Bright-field photo viewed along the [100] zone axis showing morphology of NaV_2O_5. NaV_2O_5 consists of the lamellae with an average thickness of 1 micron. There are numerous dislocations aligning parallel to the [010] direction and piling up within the marked lamellae. The corresponding electron diffraction pattern is inserted.

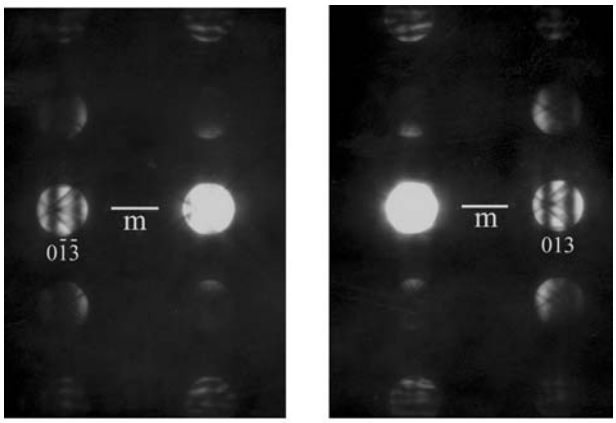

Figure 2 (a) and (b) are a pair of dark-field convergent beam electron diffraction patterns showing translation symmetry of 301 and $\bar{3}0\bar{1}$ discs, which indicates the presence of inversion center in this material.

3.2. Determination of coincident site lattice

A small misorientation between the lamellae was found by electron diffraction. By carefully adjusting these lamellae along the exact [100] zone axis, misorientations between these lamellae were determined. The detected angles were not larger than 10°. As an example, the angles between the marked lamellae in Fig. 1 were measured to be $\sim$5° (lamella I and II), $\sim$4° (lamella II and III), and $\sim$1° (lamella I and III). The twisting angles between these neighboring lamellae may not necessarily be exactly the same, but variation of these angles is very small. Also, the twist between these lamellae is not in a chirality way. The direction parallel to the normal of the grain boundary was observed in order to reveal details of the grain boundary between two lamellae. As the electron beam passes a crystalline substance, it is scattered into a number of distinct beams with small orientation differences of around two degrees according to Bragg's law. These scattered beams form a diffraction pattern at the back focal plane of the objective lens. Geometrically, the diffraction pattern is coincident with a reciprocal lattice plane in the case of single crystal. The scattered beams may also act as incident beams that can be scattered again in the specimen, resulting in a so-called double diffraction. When a polycrystalline sample is analyzed, its diffraction pattern would consist of various reciprocal lattice planes. Because of this multi-diffraction mechanism, polycrystalline specimens may produce very complex diffraction pattern which can make it difficult to interpreting the diffraction data. In

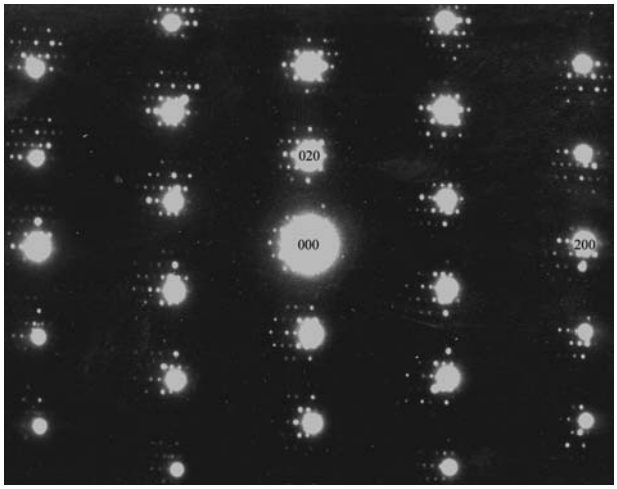

Figure 3 Electron diffraction pattern taken along the [001] zone axis shows a group of satellite reflections around every main reflection. These extra reflections are due to overlap of the bicrystals with highly orientated [001] direction.

order to correctly analyze the electron diffraction pattern, it is necessary to distinguish satellite reflections due to double diffraction from structural alternations. Fig. 3 is an electron diffraction pattern from bicrystal sharing [001] axis, but misoriented by a small angle within the (001) plane. This figure clearly shows that every main reflection has a group of satellite reflections around them due to multi diffraction. Due to relative twisting between the neighboring lamellae the rows of the satellite reflections are not parallel to that of main reflections and formation of pure twist grain boundary between the two lamellae can be predicted [18].

Careful analysis shows that the angle between rows of the satellite and main reflections is about 2.6 degree. Usually such grain boundaries can be analyzed geometrically using the concept of Coincident Site Lattice (CSL) developed by Grimmer *et al*. [19], although this concept is developed based on cubic symmetry system. CSL is formed by those lattice points that are coincident when the two misoriented lattices of neighboring grains are allowed to interpenetrate. In real space this CSL lattice is described by a parameter Σ where $1/\Sigma$ of the lattice points are common to both lattices and Σ is an odd integer. In reciprocal space, the satellite reflections resulting from multi diffraction form a superlattice called Displacement Shift Completely Lattice (DSCL) which has a reciprocal relationship with the CSL. The superlattice has the same geometrical configuration as that of the main reflections but with a rotation of $\sim 87.4^\circ$ measured in diffraction pattern. Its dimensions are $a' = 0.08$ and $b' = 0.255\ \mathrm{nm}^{-1}$, which correspond to a cell's edges of 12.2 and 3.9 nm, respectively, in real space. The relative rotation angle θ between two parallel grains is calculated based on Fig. 4. Lines OA is perpendicular to AB. OO′ is perpendicular to AA′ and equally divides θ. Because $\angle \mathrm{OAA}' + \delta = 90^\circ$ and $\angle \mathrm{OAA}' + \theta/2 = 90^\circ, \delta = \theta/2$ and θ equals two times δ. θ, (i.e. $2 \times 2.6^\circ = 5.2^\circ$), is the angle of the row of satellite reflections twisting with respect to the main reflections. Based on a number-theoretical method the angle between two sets of lattice vectors,

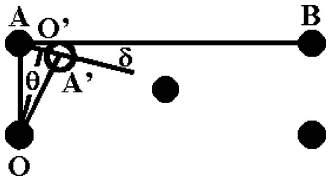

Figure 4 A schematic drawing shows the relation of relative rotation angle θ of two overlapped grains and the angle δ between the main reflections and satellite reflections rows. Solid and open circles represent the reflections from top and bottom crystals respectively.

[1 67 0], [$\bar{1}$ 67 0] and [7$\bar{1}$ 0], [710], was found to be 5.2°, thus, orientation of the basis ($a'b'c'$) of this CSL with respect to grain I and II can be calculated. The orientation relationship between the coincident lattice and host crystals at two sides of the grain boundary are a'//[1 67 0]$_{\mathrm{I}}$//[$\bar{1}$ 67 0]$_{\mathrm{II}}$, b'//[7 $\bar{1}$ 0]$_{\mathrm{I}}$// [710]$_{\mathrm{II}}$, c'//[001]$_{\mathrm{I\,or\,II}}$. If the misorientation angle between the two lamellae slightly deviates from the exact twisting value of CSL in Fig. 3, a so-called secondary dislocation could have been introduced at the grain boundary. In this case, Burgers vectors of lattice dislocation reduce to a fraction of the lattice dislocation of the corresponding CSL, resulting in lower boundaries energy [20, 21].

Construction of the CSL can be described in Fig. 5a and b. After a relative rotation of two crystals around the common origin by 5.2° within the (001) plane, the lattice points [1 67 0] and [7$\bar{1}$ 0] in grain I will coincide with the lattice points [$\bar{1}$ 67 0] and [710] in grain II. This coincidence results in the formation of the CSL with the primary orthorhombic symmetry and cell parameters of $(a^2 + 4489b^2)^{1/2}$ and $(49a^2 + b^2)^{1/2}$. The cell's volume divided by the volume of the host crystal is 470, and Σ is determined to be 235. The parameters of DSCL could also be deduced to be $(a^2 + 4489b^2)^{-1/2}$ and $(49a^2 + b^2)^{-1/2}$ based on the reciprocal relation with CSL. In orthorhombic system the reported CSL orientations are considerably smaller than those in cubic structures due to differences in the cell's edge dimensions. The smaller CSL orientations may result in high Σ value.

Fig. 6 is the corresponding bright-field photo showing morphology of the Σ235 [001] twist boundary,

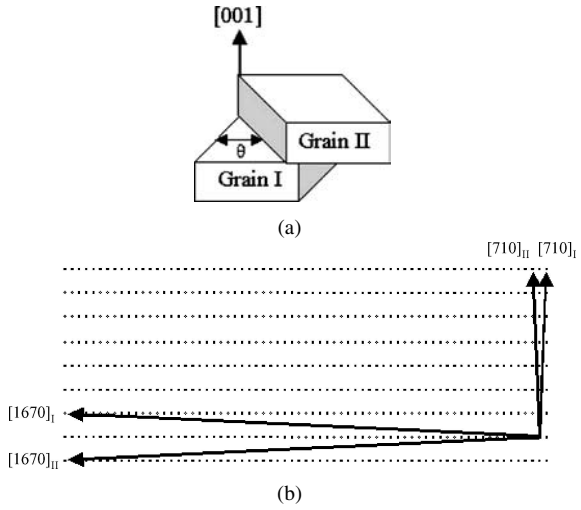

Figure 5 (a) A schematic diagram of the twist boundary formed by rotation of two crystals around the common [001] axis; (b) the outlined lattice vectors in crystal I and II for construction of the Σ235 [001] CSL.

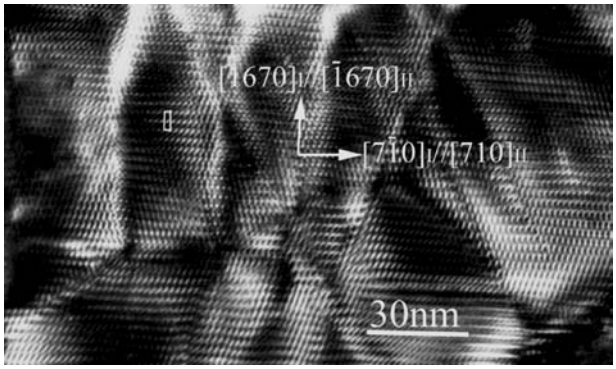

Figure 6 The corresponding bright-field micrograph showing the morphology of CSL as outlined in white lines due to Moiré effect. The Moiré effect results from the interference of the reflections from two overlapped crystals.

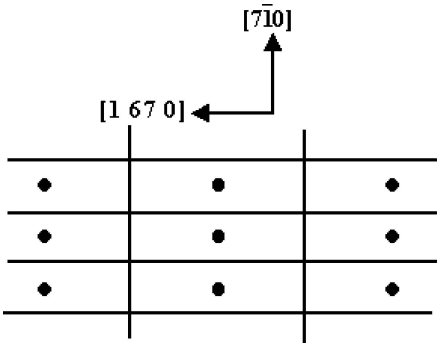

Figure 7 A schematic drawing shows the possible dislocation network within the Σ235 [001] twist boundary predicted using O-lattice theory. Solid circles represent O-lines viewed along [001] direction. The lines around each O-line indicate the predicted dislocation network.

where the dotted pattern with large distances occurs as a result of Moiré effect. The Moiré effect introduces a complex modulation resulting from interference of the reflections from two overlapping crystals. It enlarges the planar distance to be resolvable and distorts the relative orientation of the images of adjacent planes. The dimensions of the CSL (outlined with white lines) measured in this image match with the calculated values. Many defects are visible in this Moiré? image, which may correspond to the misfit dislocations at grain boundaries or to the defects shown in Fig. 1 because the twist boundary is a favorable location for initiating defects.

In order to visualize the possible dislocation network at the twist boundary O-lattice formulation has been widely used [22]. The O-lattice, $X^{(O)}$, is a sublattice of CSL and is formed by the set of elements of displacement field. It is calculated as following:

$$X_{2d}^{(O)} = 1/2 \begin{pmatrix} 1 & \frac{7a}{b} \\ -\frac{67b}{a} & 1 \end{pmatrix} \cdot \begin{pmatrix} 1 & 0 \\ 0 & 1 \end{pmatrix} \qquad (1)$$

Equation 1 represents positions (O-lines) of minimum energy for the region where atoms are located with good match at the boundary. The O lines are separated by regions where the atoms have higher energy, i.e., regions of bad match due to misorientation. Wigner-Seitz cells around the O-lines indicate the regions of bad match, in midst of the O-lines as shown in Fig. 7. The spacings between O-lines are given by $1/2(a^2 + 4489b^2)]$ and $1/2(49a^2 + b^2)$ respectively, half the cell's edges of CSL.

Charge ordering below transition temperature is parallel to *b* axis, i.e. parallel to the twist boundary. Therefore, the twist boundary does not interrupt such a charge ordering. The transition temperature of NaV_2O_5 is very sensitive to Na deficiency. The spin-Peierls transition disappeared when the composition changed to $Na_{0.97}V_2O_5$ [7]. The twist mismatch of atoms in the top and bottom crystals can be predicted to be proportional to the distance from the O-lines to the atoms and have its maximum value at the positions near the central points between the two neighbouring O-lines. The distortion of VO_5 square pyramids can only exist at the grain boundary and can not extend into the crystal. Large distortion of VO_5 square pyramids could be unfavorable for Na sitting between these distorted pyramids. As a result, deviation from the exact stoichiometric of NaV_2O_5 may happen locally at the grain boundary, although the deviation may be very small. The deviation in the composition at very localized position is expected to have very little effect on the macrophysical properties of the grown crystal since the transition temperature of the crystal remains unchanged at 35 K.

4. Conclusion

NaV_2O_5 was grown by flux method and its structure was characterized. It consists of lamellae with a small misorientation of several degrees within (001) plane. Pure twist boundaries between these lamellae were observed. A twist boundary coincident with a CSL orientation with high Σ value of 235 has been estimated. At temperatures below transition temperature, the boundaries do not interrupt the charge ordering of V^{4+} chain or ladder, because the V^{4+} chain or ladder extends along the [010] direction. Such lamellar structure may introduce deviation in the composition from the stoichiometry at a very localized position due to distortion of VO_5 square pyramids that occurred near the twist boundaries. These very localized defects are expected to have very little effect on the macroscopic properties of the grown crystal because the transition temperature was found to be unchanged.

Acknowledgements

This work was supported by National Nature Sciences Foundation of China under the NNSFC grant 60271028.

References

1. P. A. CARPY and J. GALY, *Acta Cryst. B* **31** (1975) 1481.
2. J. C. BOULOUX and J. GALY, *J. Solid State Chem.* **16** (1976) 385.
3. J. C. BOULOUX, I. MILOSEVIC and J. GALY, *ibid.* **16** (1976) 393.
4. K. WALTERSSON and B. FORSLUND, *Acta Cryst. B* **33** (1977) 789.

5. D. N. ANDERSON and R. D. WILLETT, *ibid.* **27** (1971) 1476.
6. Y. UEDA,*Chem. Mater.* **10** (1998) 2653.
7. M. ISOBE, C. KAGAMI and Y. UEDA, *J. Cryst. Grow.* **181** (1997) 314.
8. M. HASE, I. TERASAKI and K. UCHINOKURA, *Phys. Rev. Lett.* **70** (1993) 3651.
9. M. BAENNITZ, C. GEIBEL, M. DISCHNER, G. SPARN, F. STEGLICH, H. H. OTTO, M. MEIBOHM and A. A. GIPPIUS, *Phys. Rev. B* **62** (1998) 12201.
10. R. P. BONTCHEV, A. J. JACOBSON, M. M. GOSPODINOV, V. SKUMRYEV, V. N. POPOV, B. LORENZ, R. L. MENG, A. P. LITVINCHUK and M. N. ILIEV, *ibid.* **62** (1998) 12235.
11. J. C. BONNER and M. E. FISHER, *ibid.* **135** (1964) 610.
12. A. MEETSMA, J. L. DE BOER, A. DAMASCELLI, J. JEGOUDEZ, A. REVCOLEVSCHI and T. T. M. PALSTRA, *Acta Cryst. C* **54** (1998) 1558.
13. K. TSUDA, S. AMAMIYA, M. TANAKA, Y. NODA, M. ISOBE and Y. UEDA, *J. Phys. Soc. Jap.* **69** (2000) 1939.
14. T. YOSHIHAMA, M. NISHI, K. NAKAJIMA, N. ASO, K. KAKURAI, Y. FUJII, S. ITOH, C. D. FROST, S. M. BENNINGTON, M. ISOBE and Y. UEDA, *Phys. B: Cond. Matt.*, **281** (2000) 654.
15. H. NAKAO, K. OHWADA, N. TAKESUE, Y. FUJII, M. ISOBE, Y. UEDA, M. V. ZIMMERMANN, J. P. HILL, D. GIBBS, J. C. WOICIK, I. KOYAMA and Y. MURAKAMI, *Phys. Rev. Lett.* **85** (2000) 4349.
16. B. F. BUXTON, J. A. EADES, J. W. STEEDS and G. M. RACKHAM, *Phil. Trans. R. Soc. London* **281** (1976) 171.
17. M. TANAKA, R. SAITO and H. SEKII, *Acta Cryst. A* **39** (1983) 357.
18. Y. G. WANG, R. HØIER, S. STEINSVIK and T. NORBY, *J. Mat. Sci. Lett.* **13** (1994) 1789.
19. H. GRIMMER, W. BOLLMANN and D. H. WARRINGTON, *Acta Cryst.* A30 (1974) 197.
20. T. SCHOBER and R. W. BALLUFFI, *Phil. Mag.* **21** (1970) 109.
21. Y. G. WANG and J. TH. M. DE HOSSON, *J. Mat. Sci. Lett.* **20** (2001) 389.
22. W. BOLLMANN, "Crystal Defect and Crystalline Interfaces" (Springer, Berlin, 1970).

Received 15 October 2003
and accepted 26 October 2004